International Journal of Biological Macromolecules 180 (2021) 667–676

Contents lists available at ScienceDirect

International Journal of Biological Macromolecules

journal homepage: http://www.elsevier.com/locate/ijbiomac

Protein engineering of stable *Is*PETase for PET plastic degradation by Premuse

Xiangxi Meng [a,1], Lixin Yang [a,1], Hanqing Liu [a,1], Qingbin Li [a,b], Guoshun Xu [a], Yan Zhang [a,c], Feifei Guan [a], Yuhong Zhang [a], Wei Zhang [a], Ningfeng Wu [a,*], Jian Tian [a,*]

[a] *Biotechnology Research Institute, Chinese Academy of Agricultural Sciences, Beijing 100081, China*
[b] *State Key Laboratory of Microbial Technology, Shandong University, Qingdao, China*
[c] *College of Food Science and Technology, Agricultural University of Hebei, Baoding, Hebei Province 071001, China*

ARTICLE INFO

Article history:
Received 16 December 2020
Received in revised form 9 March 2021
Accepted 10 March 2021
Available online 19 March 2021

Keywords:
Protein engineering
Poly(ethylene terephthalate) (PET) biodegradation
*Is*PETase (PETase from *Ideonella Sakaiensis*)

ABSTRACT

Poly(ethylene terephthalate) (PET) is used widely by human beings, but is very difficult to degrade. Up to now, the PET degradation effect of PETase from *Ideonella sakaiensis* 201-F6 (*Is*PETase) variants with low stability and activity was not ideal. In this study, a mutation design tool, Premuse, was developed to integrate the sequence alignment and quantitative selection of the preferred mutations based on natural sequence evolution. Ten single point mutants were selected from 1486 homologous sequences using Premuse, and then two mutations (W159H and F229Y) with improved stability were screened from them. The derived double point mutant, W159H/F229Y, exhibited a strikingly enhanced enzymatic performance. Its T_m and catalytic efficiency values (k_{cat}/K_m) respectively increased by 10.4 °C and 2.0-fold using p-NPP as the substrate compared with wild type. The degradation activity for amorphous PET was increased by almost 40-fold in comparison with wild type at 40 °C in 24 h. Additionally, the variant could catalyze biodegradation of PET bottle preform at a mean rate of 23.4 $mg_{PET}/h/mg_{enzyme}$. This study allowed us to design the mutation more efficiently, and provides a tool for achieving biodegradation of PET pollution under mild natural environments.

1. Introduction

Poly(ethylene terephthalate) (PET) is one of the most widely distributed synthetic plastic pollutants worldwide, due to its desirable properties of durability, low-cost, massive yield and heavy usage [1]. Human-made PET has been present in the ecosystem for over 100 years [2], and is a burgeoning threat because of accelerated production [3–6]. Micro- and nanoplastics have been reported as present in animals and food products, meaning they are part of human food chains [7,8], and potentially threaten human health [9]. The presence of PET in ecosystems has provided a long time for decomposers in the biosphere to evolve to access PET as a novel carbon source. PET can also be depolymerized by several other cutinase enzymes. However, PET biodegradation catalyzed by these natural enzymes is inefficient and time-consuming [6,10–13]. Therefore, engineering of these PETases is an important issue.

Not content with the evolutionary speed of natural enzymes, several groups have worked on engineering PETases. One potential solution for this problem is the enhancement of operational temperatures of thermophilic PETases close to the PET glass transition temperature (~76 °C) [14,15]. Tournier et al. succeeded in creating an ICCG variant of LCC by saturation mutagenesis, by increasing the operational temperatures from 65 °C to 72 °C, so that it could break down PET bottle preforms [16]. Although this kind of approach provides a solution for industrialized PET recycling, it is of limited help for environmental engineering bacteria construction under mild environmental temperatures. However, the PETase produced by a strain of *Ideonella sakaiensis* (*Is*PETase) identified by Yoshida et al. [17] can degrade PET at ambient conditions. The engineering of *Is*PETase can address this problem, and several groups have reported research advances. For example, Kim's group introduced S121E/D186H/R280A into *Is*PETase, increasing the operational temperature of the variant by 10 °C and resulting in 14-fold higher PET degradation at 40 °C than the wild type [18]. *Is*PETase, however, exhibits poor durability, and most of its variants can only catalyze amorphous PET biodegradation with slightly higher enzyme activity [18–21].

Consensus protein design is a popular semi-rational design strategy for protein stability. It is based on the hypothesis that the respective consensus amino acids contribute more than the non-conserved amino acids at a specific position to the stability of the protein. The consensus design approach has been widely successful in improving the stabilities of proteins, resulting in melting temperatures increased by

* Corresponding authors.
E-mail addresses: wuningfeng@caas.cn (N. Wu), tianjian@caas.cn (J. Tian).
[1] These authors have contributed equally to this work.

https://doi.org/10.1016/j.ijbiomac.2021.03.058
0141-8130/

10–32 °C in some proteins [22]. However, the key step of the method, creating a good multiple sequence alignment (MSA) of the sequences, is a major computational challenge especially in large, diverse sequence datasets. In addition, the numerous columns in the MSA make it difficult to select the potential mutations, and mutation design using the method is generally considered more art than science [22–24].

With the arrival of big-data and expanded sample size, large numbers of genes have been sequenced from diverse environments and deposited in public databases. Multiple homologs (>1000) of most proteins can thus be easily acquired. Sequences from big-data provide us a new way to analyze residue evolution and its effect on protein structure and function. A standardized method is needed to deal with such big-data and mine the useful mutants from this naturally evolved sequence pool.

In this study, a web tool (Premuse, http://www.elabcaas.cn/pird/premuse.html) was developed to predict mutations based on natural sequence evolution. Pairwise alignment was employed to construct the ideal alignment and avoid the calculations required for MSA. The calculated position-specific amino acid probabilities (PSAP) were used to quantitatively select the preferred mutations. A series of evaluation criteria was introduced to establish a procedure and applied to the enzyme *Is*PETase. The W159H/F229Y derived from Premuse exhibited excellent enzymatic properties. Its melting temperature increased by 10.4 °C, and its value of k_{cat}/K_m and half-life were respectively twice and three times as much as that of wild type. As a result, the variant could catalyze biodegradation of PET bottle preform in 24 to 72 h, at a mean rate of 23.4 $mg_{PET}/h/mg_{enzyme}$, and it outperformed most of the other variants of *Is*PETase reported so far, which could only depolymerize amorphous or low-crystalline PET.

W159H/F229Y was screened from only ten alternative variants. The excellent success rate was because the strategy took full advantage of evolutionary information contained in homologous protein sequences [22]. Premuse could be an exquisite and efficient option for protein engineering with a high success rate but a low workload.

2. Materials and methods

2.1. Computational design of IsPETase by Premuse

The sequence information of poly(ethylene terephthalate) hydrolases (PETase) *Is*PETase (Accession NO: 6EQD_A) and its 1486 homologs (identity >45%, coverage >50%) were acquired from databases of NCBI. The pairwise alignment tool, needle in EMBoss [25], was used to carry out the sequence alignment between the target sequence and each of the similar proteins. All of the homologs were trimmed to the same length as and aligned to the target sequence. Then the aligned homologs were weighted and the position-specific amino acid probabilities (PSAP) of the target sequence were calculated [26]. If the evolutionary selection probability of the mutation was greater than 65% of the probability of the wild type, the amino acids were selected for the variant's construction. The above mutation selection protocol was integrated as a web tool, Premuse (Premuse, http://www.elabcaas.cn/pird/premuse.html), to design the potential mutations.

2.2. Plasmids construction

The nucleotide sequences encoding signal peptides predicted with SignalP [27] (http://www.cbs.dtu.dk/services/SignalP/) were removed. Then the gene encoding *Is*PETase was commercially synthesized with codon optimization by GenScript Co. Ltd. (Nanjing, China) and cloned into the *Hind*III and *Nco*I sites of pET-27b.

2.3. Variant construction

The single point mutations were cloned into *Is*PETase by amplifying full-length plasmid using Phanta Max Super-Fidelity DNA Polymerase (Vazyme, Nanjing, China) with partially overlapping oligonucleotides. The product of polymerase chain reaction (PCR) was circularized by homologous recombination using ClonExpress II One Step Cloning Kit (Vazyme, Nanjing, China) and transformed in *E. coli* BL21 (DE3). The DNA sequencing of variants was carried out by TSINGKE Co. Ltd. (Beijing, China). The sequences of *Is*PETase and *Is*PETase$^{W159H/F229Y}$ were also cloned into the *Hind*III and *Nco*I sites of pET-30a for large scale protein production. The primers used for cloning and site-directed mutagenesis are listed in Table S1.

2.4. Protein expression and purification

A single clone of *E. coli* BL21 (DE3) cells containing the gene of a variant was inoculated in 5 mL LB medium with 50 μg/mL kanamycin at 37 °C, 220 rpm. Then the overnight culture was grown in LB medium with 50 μg/mL kanamycin at 37 °C for 2 h to OD_{600} 0.8–1.0, and then induced by 0.4 mM isopropyl β-D-thiogalactopyranoside (IPTG) at 16 °C, 180 rpm for a further 20 h. The *E. coli* BL21 (DE3) cells were harvested by centrifugation (7000 ×*g*, 5 min, 4 °C), and washed twice and suspended by binding buffer (50 mM Tris-HCL, 0.5 M NaCl, 5 mM imidazole, pH 9.5). Then the cells were disrupted by ultrasonication. The cell precipitates were removed by centrifugation (12,000 ×*g*, 30 min, 4 °C) and filtration (0.45-μm filter, Φ25mm, JINTENG). The supernatant was applied to a Ni-NTA affinity column (Solarbio, Beijing) at 4 °C, then washed with binding buffer followed by wash buffer (50 mM Tris-HCl, 0.5 M NaCl, 50 mM imidazole, pH 9.5). The target protein was eluted with elution buffer (50 mM Tris-HCl, 0.5 M NaCl, 500 mM imidazole, pH 9.5). The eluted fraction was applied to a dialysis membrane to wash out the imidazole in dialysis buffer (50 mM Tris-HCL, 0.5 M NaCl, pH 9.5) at 4 °C. After concentration with PEG 8000, the purified enzyme was stored in storage buffer (50 mM Tris-HCL, 0.5 M NaCl, 20%(v/v) glycerol, pH 9.5) at −80 °C. Protein concentration was measured by using a BCA Protein Assay Kit (CWBIO, Beijing).

2.5. Variants screen and evaluation by p-nitrophenyl palmitate (p-NPP) colorimetric assay

The PETase catalyzed ester bond hydrolysis resulted in PET depolymerization, so that the ester bond of *p*-nitrophenyl palmitate hydrolysis could be used for fast screening of variants. The purified protein solution (0.05 mg/mL, 2.5 μL) was incubated at 50 °C for 30 min, then added into 187.5 μL of 50 mM Tris buffer (pH 9.5) with 10 μL of p-NPP solution (8 mM). After incubation for 10 min, 50 μL of 10% (m/v) TCA was added to stop the reaction, and 50 μL of 10% (m/v) Na_2CO_3 was added as a chromogenic agent. A total of 200 μL of supernatant separated by centrifugation was injected in a thin-walled 96-well PCR plate. The production of p-nitrophenol (p-NP) was detected from the absorption at 410 nm in a multiscan spectrophotometer (SpectraMax M2, Molecular Devices, US).

2.6. Analytical assessment of melting temperature

Thermal stability of *Is*PETase and variants was determined by temperature melting curves in differential scanning calorimetry (MicroCal VP-Capillary DSC System, UN). Protein in storage buffer (~0.5 mg/mL, 400 μL) was monitored by increasing temperature from 25 to 90 °C at a scanning rate of 200 °C/h. Melting temperature was determined from the first thermal shift curve.

2.7. Analysis for thermostability of variants

The variant proteins in storage solution (0.05 mg/mL) were incubated at 50 °C for 0, 5, 15, 30 and 60 min, and the residual activity was measured by *p*-nitrophenyl palmitate (p-NPP) colorimetric assay as stated above. The activity of enzyme without heat treatment was defined as 100%.

2.8. Analysis for the effects of temperature and pH on enzyme activity

The optimum temperatures of variants were determined at temperatures ranging from 25 °C to 60 °C in 50 mM Tris-HCl (pH 9.5). The optimum pH of variants was measured in 50 mM glycine-NaOH with pH ranging from 8.5 to 10.5. The activity was determined by using a *p*-nitrophenyl palmitate (p-NPP) colorimetric assay.

2.9. Kinetic analysis of variants for p-NPP

Variant proteins (1.09 μM) were incubated in 50 mM Tris-HCl (pH 9.5) with 0.08, 0.2, 0.3, 0.4, 0.6, 0.8, 1, and 1.2 μM at 40 °C. The p-NP produced was detected by a multiscan spectrophotometer as mentioned above. Initial rates were plotted against p-NPP concentrations and the kinetic parameters were determined by using the Michaelis–Menten equation in Graph Pad Prism version 6 (GraphPad Software, San Diego, CA).

2.10. Enzyme assays for BHET

The purified protein solution (14 mg/mL, 0.1 μL) was added into 190 μL of 50 mM Tris buffer (pH 9.5) with 10 μL of BHET solution (9 mM). After incubation for 5 min at 40 °C, the reaction was terminated by adding 100 μL methyl alcohol. The reaction mixture was then analyzed by HPLC, after centrifugation (10,000 ×*g*, 5 min) and filtering (0.22 μm).

2.11. Enzyme assays for amorphous PET floccule

A Coca Cola bottle was cut into PET tablets (⌀6 mm, 10 mg), then dissolved in 0.5 mL of 1,1,1,3,3,3-hexafluoro-2-propanol. A total of 20 μL of this solution was added to 165 μL reaction buffer (50 mM Tris-HCL, 20% (v/v) glycerol, pH 9.5), to generate amorphous PET floccule. Variant proteins (15 μL, 14 mg/mL) were added for PET degradation. After incubation at 40 °C for 24 h, the reaction was terminated by adding 100 μL methyl alcohol. After centrifugation (10,000 ×*g*, 5 min) and filtering (0.22 μm), the reaction mixture was analyzed by HPLC.

2.12. HPLC analysis

HPLC analysis was performed on a 1200 series HPLC system (Agilent Technologies, Santa Clara, CA, USA) equipped with a SunFire™ C18 column (5 μm, 44.6 × 250 mm, Waters, Massachusetts, USA). The column was developed with solvent A (ddH_2O with 0.1% (v/v) trifluoroacetic acid) and methyl alcohol at a flow rate of 0.8 mL/min. The percentage of methyl alcohol was changed using a linear gradient from 1% to 5% over 0–5 min, and from 5% to 100% over 5–15 min. The detection wavelength was 240 nm.

2.13. Enzyme assays for bottle grade PET preform

A Coca Cola bottle was cut into PET tablets (⌀6 mm, 10 mg), then melted using an alcohol lamp and cooled down to make PET preform. A piece of preform was soaked in 200 μL reaction buffer (50 mM Tris-HCL, 20% (v/v) glycerol, pH 9.5) with 15 μL of variant proteins (14 mg/mL). After 24 h, the weight of PET preform was measured, and the change of shape was photographed.

2.14. LC-MS analyses

HR-ESI-MS was performed on an Agilent 1260 HPLC/6520 QTOF-MS instrument (Santa Clara, CA, USA), equipped with an electrospray ionization source and a Poroshell 120 SB-C18 column (2.7 μm, 3.0 × 150 mm, Agilent, Santa Clara, CA, USA). The column was developed with solvent A (ddH_2O with 0.1% (v/v) formic acid) and methyl alcohol at a flow rate of 0.55 mL/min. The percentage of methyl alcohol was changed using a linear gradient from 5% to 40% over 1–3 min, and from 40% to 50% over 3–7 min.

2.15. Molecular docking and molecular-dynamics (MD) simulations

The wild-type *Is*PETase three-dimensional structure was retrieved from the PDB database (PDB ID: 6EQD). The three-dimensional structures of the variants were constructed with Modeler 9.22 [27]. The molecular docking consisting of *Is*PETase and 2-hydroxyethyl-(monohydroxyethyl terephthalate)$_4$ (2-HE(MHET)$_4$) was performed by AutoDock vina 1.1.2 [28]and PyMOL 1.3 [29]. The substrate conformation in the complex structures was based on previous reports [30–32].

MD simulations were carried out on wild-type and W159H/F229Y enzymes, in the free state, using the NAMD 2.12 [33] with CHARMM22 [34] force field. The procedure has been reported previously [35]. The protein structure was prepared for removing non-protein and hydrogen atoms using Discovery Studio 2.5 (https://discover.3ds.com/discovery-studio-visualizer-download). Protein molecules were placed in cubic boxes at a minimum of 12 Å distance from the edge and were solvated using TIP3P explicit water. To keep all systems neutral, 0.15 M NaCl was added. Simulations were carried out using periodic boundary conditions and a 12 Å cut-off for non-bonded interactions as well as a Particle Mesh Ewald for long-range electrostatics. A time step of 2 fs was used, and snapshots were saved every 1 ps. The protein was fully constrained, and the solvent minimized for 2000 steps using a conjugate gradient algorithm. The solvent was equilibrated for 100 ps under constant-temperature, constant-pressure NPT conditions. The solvent was then fully constrained, and the protein minimized for 2000 steps. The entire system was then minimized for another 2000 steps and equilibrated for 100 ps under the same NPT conditions. Finally, a 20-ns MD simulation was performed at 400 K in constant-energy, constant-volume ensemble NVE conditions.

2.16. Phylogenetic analysis of IsPETase mutational sites

In total, 14 full-length protein sequences of known PETases reviewed by Taniguchi et al. [36] were aligned by ClustalW. The phylogenetic analysis was performed with MEGA-X [37], and the guide tree was obtained on the basis of the neighbor-joining method using the p-distance model.

2.17. Crystallinity analyses by differential scanning calorimetry (DSC)

The crystallinity of bottle grade PET and preform were analyzed by the DSC (NETZSCH DSC 214) with the previously described method [38] at the ZHONG KE BAI CE Technology Service Company (Beijing, China). A sample of 3 mg was heated from 0 to 280 °C at 10 °C min^{-1}. The heat of PET melting ΔH_m and heat of PET cold crystallization ΔH_c were determined by integrating areas (J g^{-1}) under peaks. The heat of melting (100% crystalline PET) ΔH_m^0 is estimated to be 140.1 J g^{-1}. PET crystallinity is measured according to the following equation:

$$\%\text{crystallinity} = \left((|\Delta H_m| - |\Delta H_c|) / \Delta H_m{}^0 \right) \times 100$$

3. Results

3.1. Protein engineering for improving the stability of IsPETase using Premuse

To design potential mutations from the large number of homologs, a protocol (Fig. 1) was proposed to integrate pairwise alignment [39], sequence weighting [40], position-specific amino acid probabilities (PSAP) calculation [26], and preferred mutation selection. The sequence alignment between the target sequence and each of the similar proteins

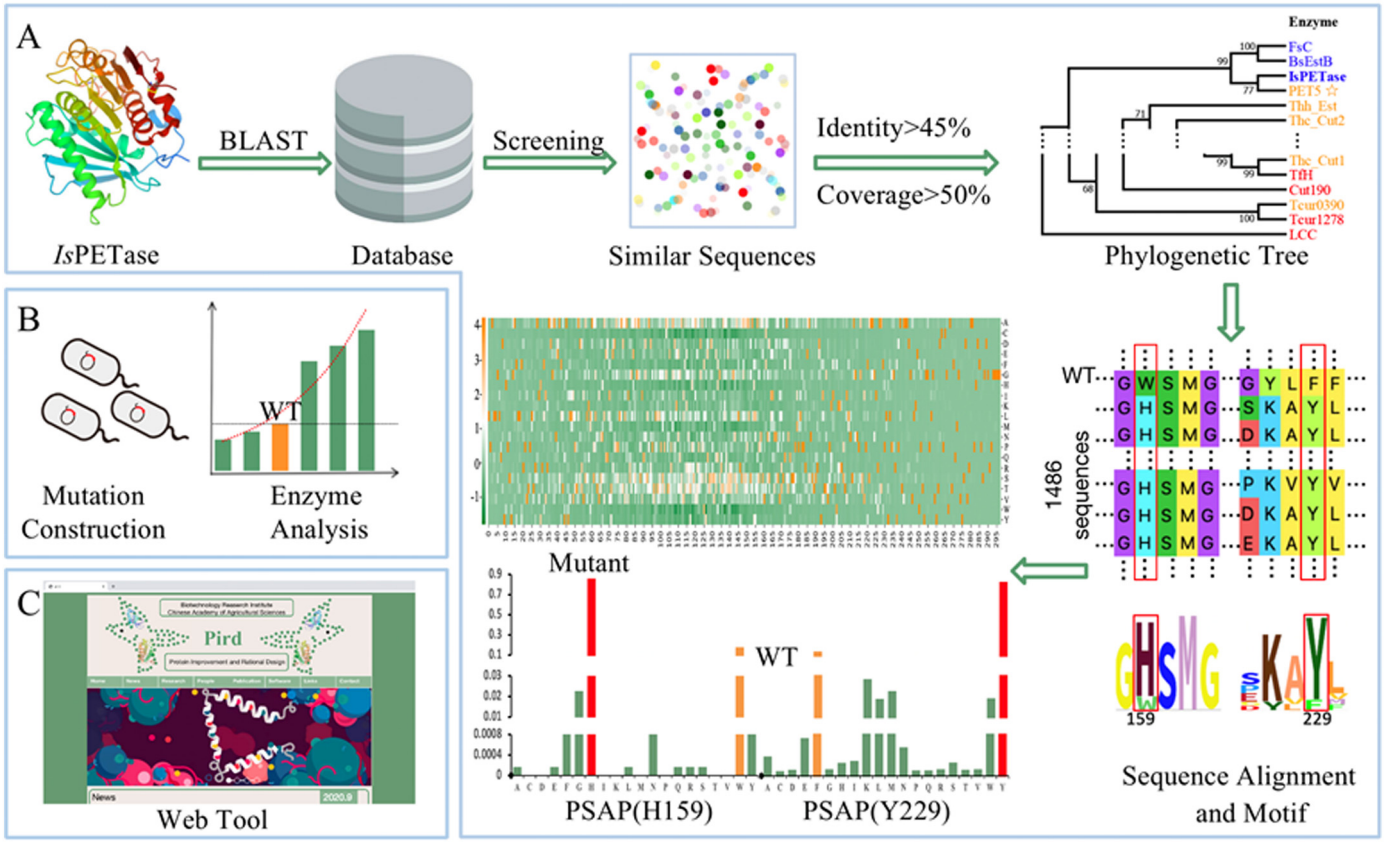

Fig. 1. Premuse protein engineering and screening approach. (A) In the design stage, 1486 *Is*PETase homologous protein sequences were collected from NCBI, and PASP was calculated using Premuse arithmetic. (B) Using a p-NPP assay, the variants were screened, and then the PET biodegradation was tested. (C) The Pird web tool was integrated with Premuse.

was calculated based on the Needleman-Wunsch alignment algorithm. The PSAP of the target sequence were calculated based on the Dirichlet mixture and sequence weighted methods. The mutations were quantitatively selected from the PSAP matrix, which has a higher probability of the mutation than the wild type. All of the calculations were integrated into a web tool (Fig. 1) to predict the mutations based on sequence evolution (Premuse, http://www.elabcaas.cn/pird/premuse.html).

To design the mutations of *Is*PETase, 1486 sequences similar to *Is*PETase with more than 40% identity and 50% coverage were obtained from NCBI [41] with the tool BLASTP suite [42]. Ten mutations with large differences in the PSAP matrix between the mutation and wild type were selected based on the calculation of Premuse and are shown in Table 1. For instance, the wild-type amino acid at position 159 was tryptophan (W), and the frequency of occurrence in the sequence alignments (Table 1) was 14.8%; however, the most highly conserved residue in the same site of homologs was histidine, at a frequency of 82.6%. It can be speculated that the function of mutation W159H could be more advantageous than wild type for maintaining structural or conformational stability of the protein.

Table 1
Premuse analysis of the stabilizing point mutations based on their frequencies of amino acids.

AA No.	Wild AA	Max AA	Frequency of Wild AA (%)	Frequency of Max AA (%)	Diff (%)
65	A	G	3.07	76.52	73.44
127	Q	L	4.75	74.95	70.20
132	R	D	2.19	71.48	69.29
134	V	L	10.47	84.62	74.14
139	G	S	3.26	68.47	65.21
154	M	L	1.61	78.81	77.20
159	W	H	14.47	82.57	68.09
169	S	A	4.77	82.95	78.18
229	F	Y	10.19	79.16	68.97
270	T	Q	1.08	70.52	69.44

3.2. Characterization of variants improved thermal stability

To evaluate the effect of the mutation on thermal stability, the genes of ten mutants and wild type were constructed in the expression plasmid pET-30a(+). The protein expression was induced overnight at 16 °C in *E. coli* strain BL21(DE3). As biodegradation of PET was time-consuming, the p-NPP colorimetric assay was carried out for preliminary variant screening and enzymatic characterization. After incubation at 50 °C for half an hour, the remaining p-NPP hydrolysis activity of variants was determined. The wild type remained at 16.5%, while the residual activities of G139S, W159H and F229Y were dramatically enhanced, at 59.2%, 78.4% and 51.5% respectively (Fig. 2A).

To further confirm the stability improvement, the T_m values of variants were also measured. The T_m value of G139S, 50.5 °C, was similar to that of wild type. In contrast, the T_m values of W159H and F229Y were 57.6 °C and 54.4 °C, which were 6.8 °C and 3.6 °C higher than the 50.8 °C of wild type (Fig. 2B).

The T_m value and residual enzyme activity of W159H and F229Y variants were higher than those of wild type, which indicated that the structure and activity of both variants were improved. Therefore, the two variants were selected to construct the combined variant W159H/F229Y. Its remaining activity was 96.0% and T_m value was 61.2 °C, indicating further substantial improvement over wild type.

In order to verify the stability improvement of W159H/F229Y, the thermo- stability and optimal temperature of variants were characterized. The residual enzyme activity of mutant W159H/F229Y was basically unchanged in the course of one hour of heat treatment at 50 °C. The mutant W159H and F229Y lost partial activity, with 78.4% and

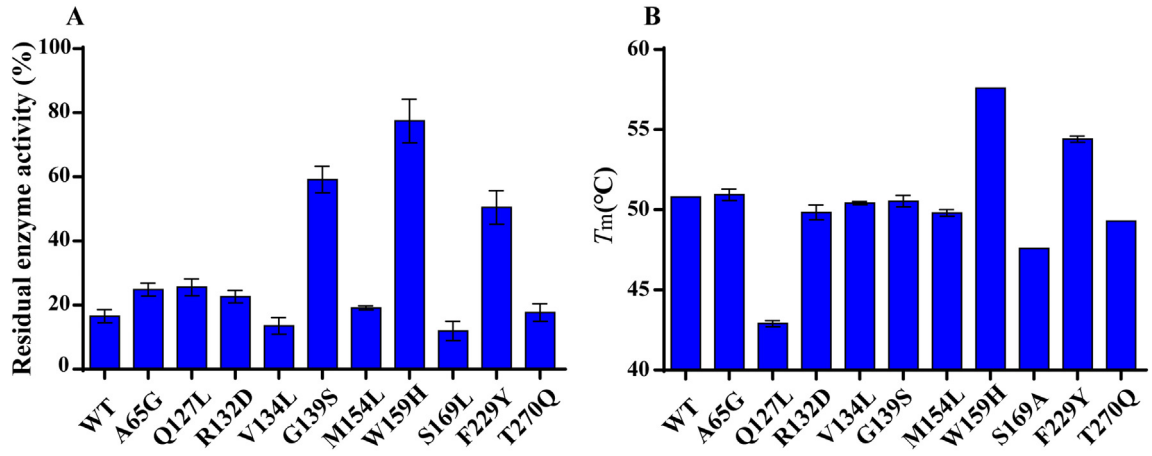

Fig. 2. Screening of the variants generated in this study. (A) Residual enzyme activity of WT and variants at 50 °C for 30 min. Experiments were performed using p-NPP colorimetric assay. (B) T_m values of WT and variants.

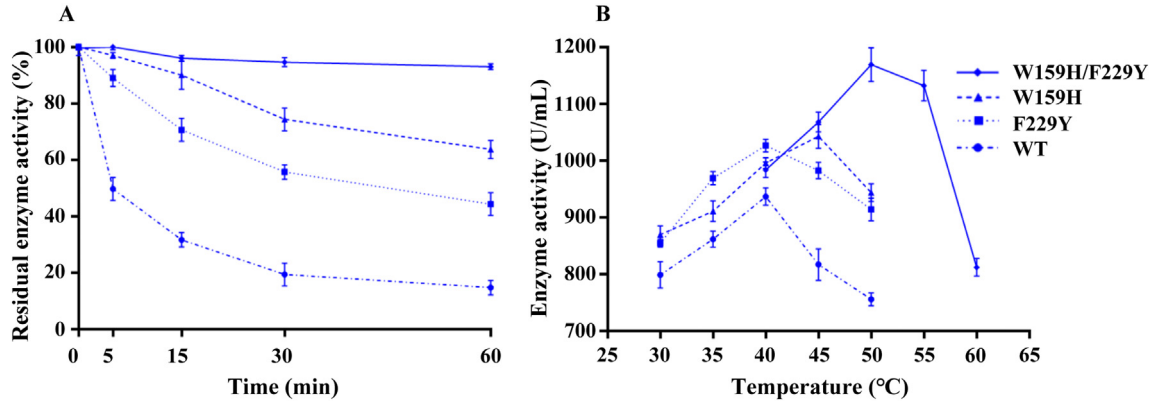

Fig. 3. Thermal stability measurements of the wild type and screened variants. (A) Residual enzyme activity of WT and variants at 50 °C for 1 h. (B) The effect of temperature on the activities of the WT and variants. Experiments were performed using p-NPP colorimetric assay.

51.5% residual enzyme activity. However, the residual enzyme activity of wild type was only 16.5%, which meant it lost most of its enzyme activity (Fig. 3A).

3.3. Temperature and pH dependency of wild type and variants

The optimal temperature of variant F229Y was the same as wild type, at 40 °C. The optimal temperature of variant W159H was 45 °C, and the optimal temperature of combined variant W159H/F229Y was 50 °C (Fig. 3B). This sharp rise in optimal temperature indicated that W159H/F229Y had good stability, which was in good agreement with the above results.

To investigate changes in physical and chemical properties caused by variants, an assay for optimal pH value was carried out. All variants had optimal enzyme activity between pH 9.0 and 9.5, and there was no visible difference among them in terms of pH (Fig. S1). The consistency in optimal pH value indicated that the change in variants was mainly higher thermal stability.

3.4. Catalytic efficiency of wild type and mutants

The catalytic efficiency of variants was also determined at 40 °C. Compared with the wild type, the kinetic parameter (k_{cat}/K_m) of W159H/F229Y for p-NPP hydrolysis was increased by 100% (Table 2), and the hydrolytic activity for bis (2-hydroxyethyl) terephthalic acid (BHET) of W159H/F229Y was 2.6 times as much as that of wild type (Fig. S2). These results showed that the catalytic efficiency of W159H/F229Y was improved.

3.5. Increased thermal stability and catalytic efficiency resulted in enhanced PET degradation activity

Long term stability measurements of wild type and W159H/F229Y were performed at 40 °C for 24 h, to ensure that the enzyme could function for a long time in the process of PET degradation. As expected, W159H/F229Y lost less enzyme activity at a slower rate than the wild type (Fig. S3). While the half-life of W159H/F229Y was 26.6 h, the half-life of wild type was only 9.7 h.

With the significantly improved performance of W159H/F229Y, the anticipated amorphous PET digestion was explored. After incubation for 24 h at 40 °C, the total concentration of released compound by W159H/F229Y had a 40-fold increase over that released by wild type (Fig. 4A). The products released by *Is*PETase, which were

Table 2
Kinetic parameters of the wild type and variants. The kinetic parameters were determined in pH 9.5 buffer at 40 °C with p-NPP colorimetric assay.

Mutant	$k_{cat}(s^{-1})$	$K_m(mmol \cdot L^{-1})$	k_{cat}/K_m $(mmol^{-1} \cdot L \cdot s^{-1})$
*Is*PETase	11.59 ± 0.16	0.19 ± 0.01	61.00 ± 0.84
W159H	6.71 ± 0.12	0.08 ± 0.01	83.88 ± 1.50
F229Y	11.25 ± 0.19	0.18 ± 0.01	62.50 ± 1.05
W159H/F229Y	9.64 ± 0.13	0.08 ± 0.01	120.50 ± 1.63

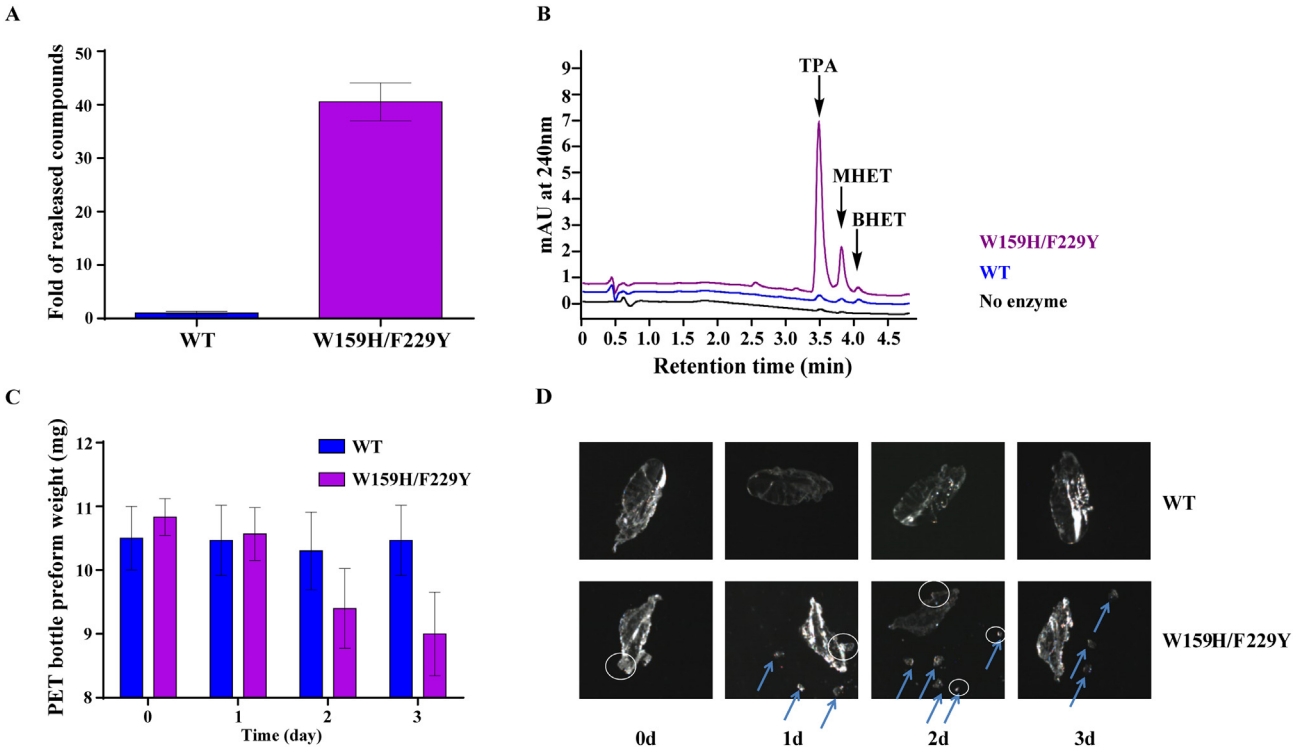

Fig. 4. Comparison of wild-type *Is*PETase and W159H/F229Y in assays of PET biodegradation. (A) Comparison of the specific hydrolytic activity of W159H/F229Y and wild-type toward amorphous PET. (B) High-performance liquid chromatography spectrum of the BHET, MHET and TPA products released from the amorphous PET. (C) Degradation of PET bottle preform by wild-type and W159H/F229Y; the weight of PET bottle preform was determined every 24 h. (D) The shape changes caused by wild-type and W159H/F229Y depolymerization. Arrows indicate exfoliated particles. Circles indicate the missing part of the main body.

terephthalic acid (TPA), mono (2-hydroxyethyl) terephthalic acid (MHET), and BHET, were identified by HPLC-HR-MS analysis (Figs. 4B and S4). This result was consistent with that reported by Yoshida *et al* [17].

The high performance of W159H/F229Y suggested that its potential applications could be extended to biodegradation for PET waste (29.2 ± 0.8% crystallinity), which causes ubiquitous pollution. The use of W159H/F229Y for decomposition of PET bottle preform (10.7 ± 0.6% crystallinity) was examined. The PET bottle preform treated by wild type displayed slight changes in shape or weight, due to the poor stability of *Is*PETase. However, the PET bottle preform lost 1.8 mg after it was treated by W159H/F229Y for 3 days, and the mean decomposition rate reached 23.4 $mg_{PET}/h/mg_{enzyme}$. Additionally, some particles clearly fell off from the main body and then disappeared due to decomposition by W159H/F229Y (Fig. 4C and D). These results therefore further inspired the enzymatic processing of PET waste.

3.6. Molecular-dynamics simulations revealed the mechanism underlying W159H/F229Y Improvement

To gain better insight into the structural effects of the mutations, molecular-dynamics simulations of the enzymes were carried out. The root mean square deviation (RMSD) of W159H/F229Y was significantly lower than that of wild type (Fig. 5A), and the number of hydrogen bonds of W159H/F229Y was significantly higher than that of wild type (Fig. 5B). A substantial difference in root mean square fluctuations (RMSF) was observed in the area of amino acid 205 to 235 (Fig. 5C), where most of the extra hydrogen bonds derived from F229Y were concentrated (Figs. 5D, S5 and S6A). As this area was near the active site, change may greatly increase protein stability. The number of salt bonds (Fig. S6B) and structural electrostatic energies (Fig. S7) were also determined by molecular dynamics simulation, but there was no obvious change between F229Y and wild type.

The substitution of histidine for tryptophan in the W159H mutation reduced the distance between residues Asp118 and Arg123 from 5.5 Å in wild type to 2.7 Å in W159H. In addition, a new salt bridge formed, which was not present in F229Y but was retained in W159H/F229Y (Fig. 6A). This was consistent with the T_m value of W159H being 2.5 °C higher than F229Y (Fig. 2B), and suggested the key molecular mechanism to improve the variant stability. However, the substitution of histidine for tryptophan in W159H mutation conferred a new salt bridge interaction between residue H159 and 2-HE(MHET)$_4$. Residue Trp185 was observed to form π-π interactions with the aromatic motif of the PET polymer (Fig. S8), which was also suggested by Cui et al. [38]. This result significantly enhanced the binding affinity for PET polymer, and could explain the lower K_m value of W159H (Table 2). All of these results indicated that W159H contributed more than F229Y to increase enzyme properties.

4. Discussion

Traditional consensus design strategies rely on manual selection of protein sequences for MSA, which limits their utilization. Premuse, the alternative to manual MSA construction is standardized for sequence alignment and quantitative selection of the preferred mutations. In the sequence alignment, Premuse only considers the alignment between the target sequence and homologs from the database, rather than the entire MSA. Therefore, the method could exponentially reduce the computation quantity, allowing it to easily deal with large datasets, and mine information from big-data. Consequently, the expanded size homologs based on big-data (1486 protein sequences) could not only reflect the results of natural evolution, but also allow for the advantages of this design strategy. As a result, this strategy could avoid the huge amount of work from saturation mutagenesis [16], and randomness of rational protein engineering [18,20], due to widespread epistatic effects and dependence on a specific structure [43–45]. Austin et al. [32]

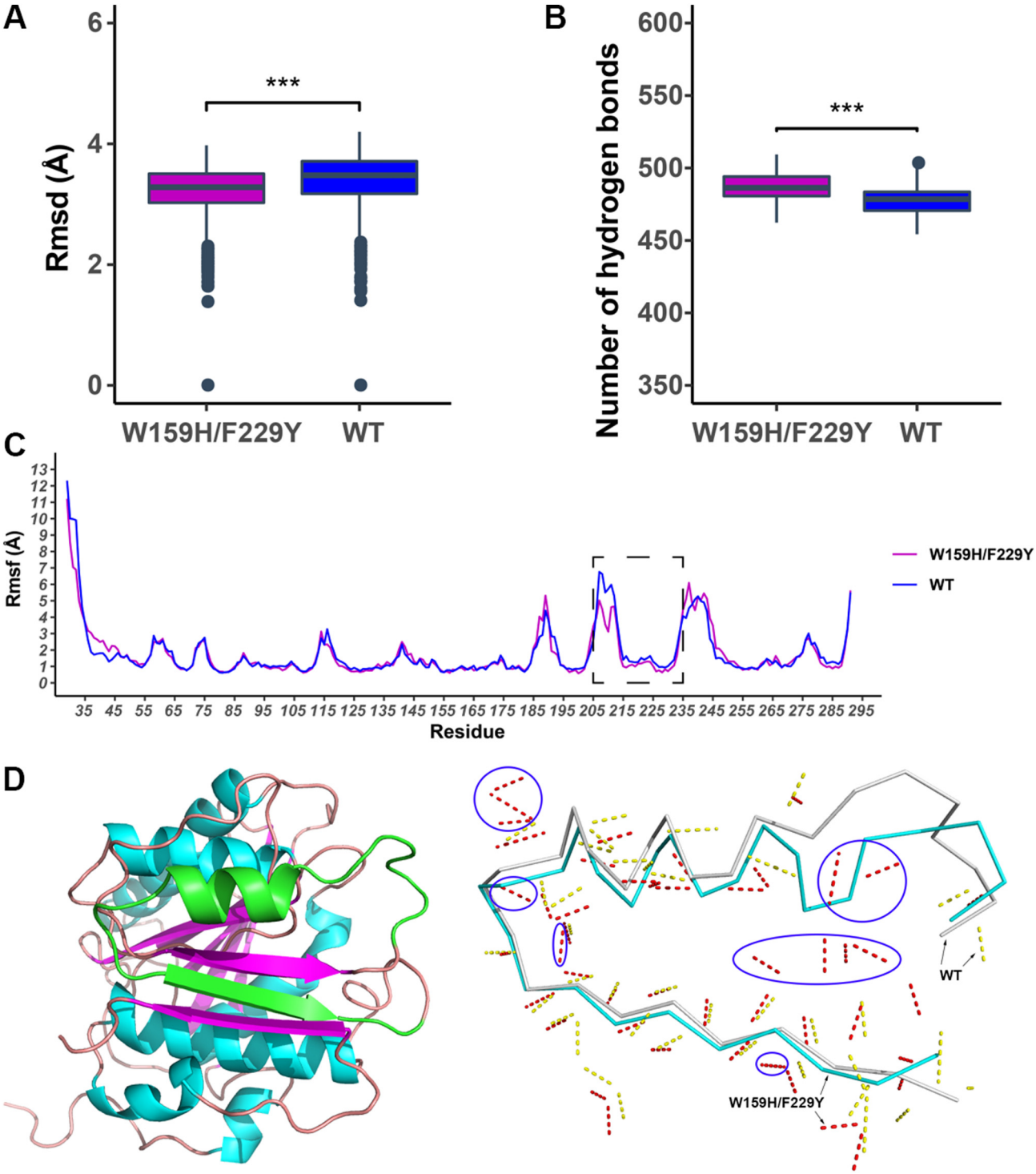

Fig. 5. Molecular-dynamics simulations carried out with WT *Is*PETase and the W159H/F229Y variant. (A) Comparison of root mean square deviation (RMSD) between W159H/F229Y and wild-type. (B) Comparison of the number of hydrogen bonds between W159H/F229Y and wild-type. (C) Comparison of protein backbone flexibility using average root mean square fluctuations (RMSF) of Cα atoms calculated per residue along molecular-dynamics simulations of enzymes. The dashed box highlights the amino acids 205 to 235 with substantial difference. (D) Hydrogen bond distribution in the region of amino acids 205 to 235. There were more hydrogen bonds (red dashed line, circled in blue) in W159H/F229Y (green) than in wild type (yellow dashed line).

produced a double mutant S238F/W159H to make *Is*PETase more cutinase-like and narrow the binding cleft, improved PET degradation was observed. Premuse also designed W159H, it indicated that the arithmetic could act as a professional designer for the protein engineering.

The p-NPP colorimetric assay used in this study avoided slow progress in decomposition of PET, which was rapid and effective for screening and characterizing *Is*PETase variants. The successful application of W159H/F229Y in PET bottle biodegradation also manifested its rationality. The MD simulations suggested the effect of mutations on stability and activity enhancement, which explained the improvement *via* a structural view.

To date, a series of enzymes have been identified as PETases biochemically, which were able to hydrolyze natural polyester and retain broad substrate specificity [36]. The stability of these PETases varied,

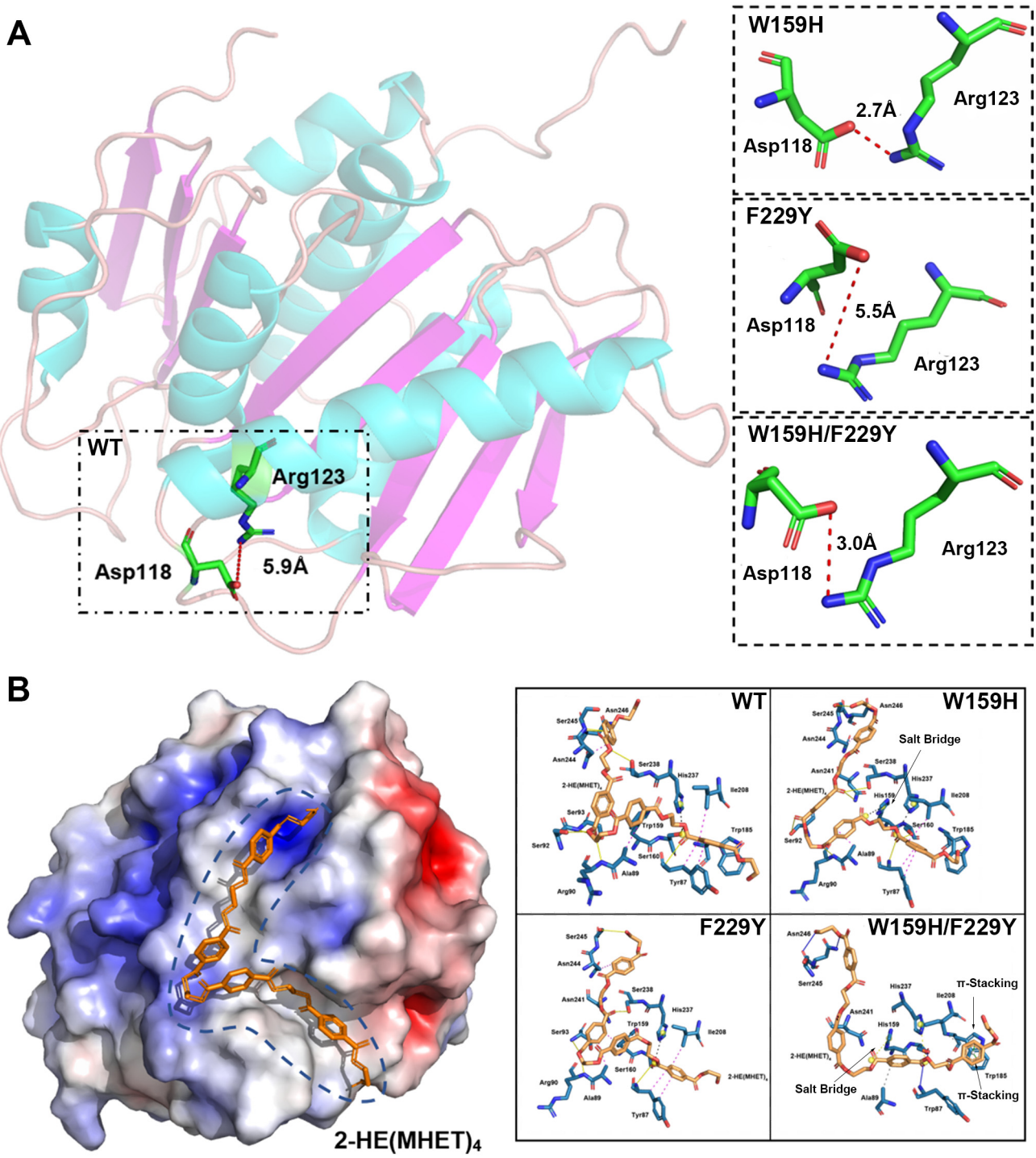

Fig. 6. Structural effects of W159H/F229Y variant. (A) The newly formed salt bridge between Asp118 and Arg123 enhanced protein stability. (B) Structural effects of W159H mutation for catalytic efficiency.

and the PETases with higher optimal temperature could be more stable, so that the MSA and phylogenetic trees could be constructed to illustrate the changes in stability over evolutionary time (Fig. 7). These PETases could be clustered into three groups with different optimal temperatures: low-temperature PETases (≤40 °C) [14,17,46], medium-temperature PETases (50–60 °C) [47–49], and high-temperature PETases (≥60 °C) [50–53]. In low-temperature PETases, the amino acid at site 159 was tryptophan (W), isoleucine (I), or tyrosine (Y) rather than histidine (H), and the amino acid at site 229 was phenylalanine (F) instead of tyrosine (Y). However, in almost all sequences from medium-temperature and high-temperature groups, the amino acid was H at site 159, and Y at site 229. Interestingly, PET5, whose optimal temperature was 50 °C, was an exception, although its amino acid at site 229 was Y, the amino acid at site 159 was W rather than H. On one hand, PET5 and *Is*PETase had a very close genetic relationship. On the other hand, PET5 was in the medium-temperature PETases group, while the optimal temperature of *Is*PETase was 40 °C. This indicated that PET5 could function transitionally in the process of evolving stability. In brief, the phylogenetic analysis also demonstrated the importance of W159H and F229Y for stability of PETases. First, the hypothesis at the basis of this strategy was accurate. Second, it meant that this strategy utilized evolutionary history and identified stabilizing features

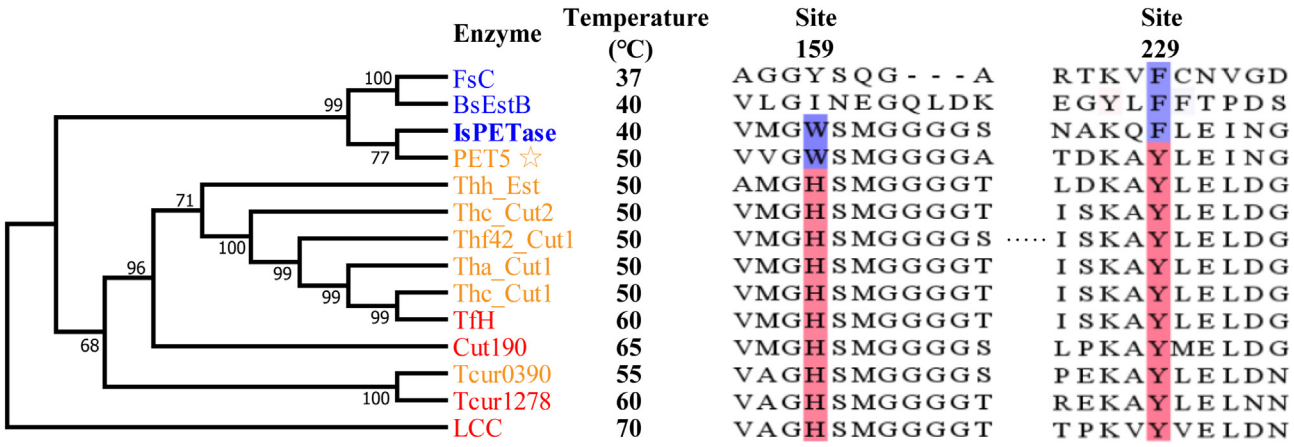

Fig. 7. Phylogenetic analysis of known PETases. *Is*PETase in this study is shown in bold. PET5, which is considered a transitional form in evolution, was marked by a star. Low-temperature PETases are in blue, medium-temperature PETases are in orange, and high-temperature PETases are in red. The residues, which were the same as the *Is*PETase, are in light blue. The stable residues are in light red. Bootstrap values are shown at the branch points.

encapsulated in homologous protein sequences. In the phylogenetic analysis, the amino acids in almost all PETases in medium-temperature and high-temperature groups were the same as W159H/F229Y, which proved the accuracy of the theory from consensus design in reverse.

In summary, using improved consensus protein engineering, W159H/F229Y-catalyzed PET bottle waste biodegradation was improved, with a mean decomposition rate of 23.4 $mg_{PET}/h/mg_{enzyme}$. The *I. sakaiensis* bacterium secretes *Is*PETase that catalyzes the degradation of PET to monomers as a carbon source for catabolization. W159H/F229Y performed well for efficient PET bottle preform degradation at a mild temperature, and provided concepts and solutions for construction of engineered bacteria in this area. Moreover, this study has demonstrated that the Premuse strategy can be very effectively utilized in protein engineering to enhance stability.

Funding

This work was supported by the Central Public-Interest Scientific Institution Basal Research Fund (Grant Number: Y2019XK19), Xinjiang Key Research and Development Program of China (Grant Number: 2018B01006-1), Central Public-Interest Scientific Institution Basal Research Fund (No. 1610392020001) and the Agricultural Science and Technology Innovation Program (ASTIP).

Ethical statement

This article does not contain any studies with human participants or animals performed by any of the authors.

CRediT authorship contribution statement

Jian Tian and Ningfeng Wu conceived and designed research. Xiangxi Meng, Lixin Yang and Hanqing Liu conducted experiments. Xiangxi Meng, Qingbin Li, Yan Zhang and Guoshun Xu contributed new reagents or analytical tools. Xiangxi Meng, Feifei Guan, Yuhong Zhang and Wei Zhang analyzed data. Xiangxi Meng and Jian Tian wrote the manuscript. All authors read and approved the manuscript.

Declaration of competing interest

None.

Appendix A. Supplementary data

Supplementary data to this article can be found online at https://doi.org/10.1016/j.ijbiomac.2021.03.058.

References

[1] V. Sinha, M.R. Patel, J.V. Patel, Pet waste management by chemical recycling: a review, J. Polym. Environ. 18 (1) (2010) 8–25, https://doi.org/10.1007/s10924-008-0106-7.
[2] U.T. Bornscheuer, Feeding on plastic, Science 351 (6278) (2016) 1154–1155, https://doi.org/10.1126/science.aaf2853.
[3] S.B. Borrelle, J. Ringma, K.L. Law, C.C. Monnahan, L. Lebreton, A. McGivern, E. Murphy, J. Jambeck, G.H. Leonard, M.A. Hilleary, M. Eriksen, H.P. Possingham, H. De Frond, L.R. Gerber, B. Polidoro, A. Tahir, M. Bernard, N. Mallos, M. Barnes, C.M. Rochman, Predicted growth in plastic waste exceeds efforts to mitigate plastic pollution, Science 369 (6510) (2020) 1515–1518, https://doi.org/10.1126/science.aba3656.
[4] P. Villarrubia-Gómez, S.E. Cornell, J. Fabres, Marine plastic pollution as a planetary boundary threat – the drifting piece in the sustainability puzzle, Mar. Policy 96 (2018) 213–220. doi:https://doi.org/10.1016/j.marpol.2017.11.035.
[5] S. Selke, R. Auras, T.A. Nguyen, E. Castro Aguirre, R. Cheruvathur, Y. Liu, Evaluation of biodegradation-promoting additives for plastics, Environ. Sci. Technol. 49 (6) (2015) 3769–3777, https://doi.org/10.1021/es504258u.
[6] R. Wei, W. Zimmermann, Microbial enzymes for the recycling of recalcitrant petroleum-based plastics: how far are we? Microb. Biotechnol. 10 (6) (2017) 1308–1322, https://doi.org/10.1111/1751-7915.12710.
[7] K. Wang, J. Li, L. Zhao, X. Mu, C. Wang, M. Wang, X. Xue, S. Qi, L. Wu, Gut microbiota protects honey bees (Apis mellifera L.) against polystyrene microplastics exposure risks, J. Hazard. Mater. 402 (2021), 123828, https://doi.org/10.1016/j.jhazmat.2020.123828.
[8] M. Kosuth, S.A. Mason, E.V. Wattenberg, Anthropogenic contamination of tap water, beer, and sea salt, PLoS One 13 (4) (2018), e0194970, https://doi.org/10.1371/journal.pone.0194970.
[9] B. Toussaint, B. Raffael, A. Angers-Loustau, D. Gilliland, V. Kestens, M. Petrillo, I.M. Rio-Echevarria, G. Van den Eede, Review of micro- and nanoplastic contamination in the food chain, Food Addit. Contam., Part A 36 (5) (2019) 639–673, https://doi.org/10.1080/19440049.2019.1583381.
[10] T. Brueckner, A. Eberl, S. Heumann, M. Rabe, G.M. Guebitz, Enzymatic and chemical hydrolysis of poly(ethylene terephthalate) fabrics, J. Polym. Sci., Part A: Polym. Chem. 46 (19) (2008) 6435–6443, https://doi.org/10.1002/pola.22952.
[11] M.A.M.E. Vertommen, V.A. Nierstrasz, M.v.d. Veer, M.M.C.G. Warmoeskerken, Enzymatic surface modification of poly(ethylene terephthalate), J. Biotechnol. 120 (4) (2005) 376–386, https://doi.org/10.1016/j.jbiotec.2005.06.015.
[12] R. Wei, D. Breite, C. Song, D. Gräsing, T. Ploss, P. Hille, R. Schwerdtfeger, J. Matysik, A. Schulze, W. Zimmermann, Biocatalytic degradation efficiency of postconsumer polyethylene terephthalate packaging determined by their polymer microstructures, Adv. Sci. 6 (2019)https://doi.org/10.1002/advs.201900491.
[13] F. Kawai, T. Kawabata, M. Oda, Current knowledge on enzymatic PET degradation and its possible application to waste stream management and other fields, Appl. Microbiol. Biotechnol. 103 (11) (2019) 4253–4268, https://doi.org/10.1007/s00253-019-09717-y.
[14] Å.M. Ronkvist, W. Xie, W. Lu, R.A. Gross, Cutinase-catalyzed hydrolysis of poly(ethylene terephthalate), Macromolecules 42 (14) (2009) 5128–5138, https://doi.org/10.1021/ma9005318.
[15] W. Zimmermann, S. Billig, Enzymes for the biofunctionalization of poly(ethylene terephthalate), Adv. Biochem. Eng. Biotechnol. 125 (2011) 97–120. doi:https://doi.org/10.1007/10_2010_87.
[16] V. Tournier, C.M. Topham, A. Gilles, B. David, C. Folgoas, E. Moya-Leclair, E. Kamionka, M.L. Desrousseaux, H. Texier, S. Gavalda, M. Cot, E. Guémard, M. Dalibey, J. Nomme, G. Cioci, S. Barbe, M. Chateau, I. André, S. Duquesne, A. Marty, An engineered PET depolymerase to break down and recycle plastic bottles, Nature 580 (7802) (2020) 216–219, https://doi.org/10.1038/s41586-020-2149-4.
[17] S. Yoshida, K. Hiraga, T. Takehana, I. Taniguchi, H. Yamaji, Y. Maeda, K. Toyohara, K. Miyamoto, Y. Kimura, K. Oda, A bacterium that degrades and assimilates poly

(ethylene terephthalate), Science 351 (6278) (2016) 1196–1199, https://doi.org/10.1126/science.aad6359.
[18] H.F. Son, I.J. Cho, S. Joo, H. Seo, H.-Y. Sagong, S.Y. Choi, S.Y. Lee, K.-J. Kim, Rational protein engineering of thermo-stable PETase from *Ideonella sakaiensis* for highly efficient PET degradation, ACS Catal. 9 (4) (2019) 3519–3526, https://doi.org/10.1021/acscatal.9b00568.
[19] A.M. de Castro, A. Carniel, J. Nicomedes Junior, A. da Conceição Gomes, É. Valoni, Screening of commercial enzymes for poly(ethylene terephthalate) (PET) hydrolysis and synergy studies on different substrate sources, J. Ind. Microbiol. Biotechnol. 44 (6) (2017) 835–844, https://doi.org/10.1007/s10295-017-1942-z.
[20] B. Liu, L. He, L. Wang, T. Li, C. Li, H. Liu, Y. Luo, R. Bao, Protein crystallography and site-direct mutagenesis analysis of the poly(ethylene terephthalate) hydrolase PETase from *Ideonella sakaiensis*, ChemBioChem 19 (14) (2018) 1471–1475, https://doi.org/10.1002/cbic.201800097.
[21] Y. Ma, M. Yao, B. Li, M. Ding, B. He, S. Chen, X. Zhou, Y. Yuan, Enhanced poly(ethylene terephthalate) hydrolase activity by protein engineering, Engineering 4 (6) (2018) 888–893, https://doi.org/10.1016/j.eng.2018.09.007.
[22] B.T. Porebski, A.M. Buckle, Consensus protein design, Protein. Eng. Des. Sel. 29 (7) (2016) 245–251, https://doi.org/10.1093/protein/gzw015.
[23] D.A. Morrison, M.J. Morgan, S.A. Kelchner, Molecular homology and multiple-sequence alignment: an analysis of concepts and practice, Aust. Syst. Bot. 28 (1) (2015) 46–62, https://doi.org/10.1071/SB15001.
[24] C. Kemena, C. Notredame, Upcoming challenges for multiple sequence alignment methods in the high-throughput era, Bioinformatics 25 (19) (2009) 2455–2465, https://doi.org/10.1093/bioinformatics/btp452.
[25] S.A. Olson, Emboss opens up sequence analysis, Brief. Bioinformatics. 3 (1) (2002) 87–91, https://doi.org/10.1093/bib/3.1.87.
[26] V.-A. Nguyen, J. Boyd-Graber, S.F. Altschul, Dirichlet mixtures, the Dirichlet process, and the structure of protein space, J. Comput. Biol. 20 (1) (2013) 1–18, https://doi.org/10.1089/cmb.2012.0244.
[27] B. Webb, A. Sali, Comparative protein structure modeling using MODELLER, Curr. Protoc. Bioinformatics 47 (5.6) (2014) 1–32, https://doi.org/10.1002/0471250953.bi0506s47.
[28] O. Trott, A.J. Olson, AutoDock Vina: improving the speed and accuracy of docking with a new scoring function, efficient optimization, and multithreading, J. Comput. Chem. 31(2) (2010) 455–461. doi:https://doi.org/10.1002/jcc.21334.
[29] B.H.M. Mooers, Shortcuts for faster image creation in PyMOL, Protein Sci. 29 (4) (2020).
[30] S. Joo, I.J. Cho, H. Seo, H.F. Son, H.-Y. Sagong, T.J. Shin, S.Y. Choi, S.Y. Lee, K.-J. Kim, Structural insight into molecular mechanism of poly(ethylene terephthalate) degradation, Nat. Commun. 9 (1) (2018), 382, https://doi.org/10.1038/s41467-018-02881-1.
[31] X. Han, W. Liu, J.-W. Huang, J. Ma, Y. Zheng, T.-P. Ko, L. Xu, Y.-S. Cheng, C.-C. Chen, R.-T. Guo, Structural insight into catalytic mechanism of PET hydrolase, Nat. Commun. 8 (1) (2017), 2106, https://doi.org/10.1038/s41467-017-02255-z.
[32] H.P. Austin, M.D. Allen, B.S. Donohoe, N.A. Rorrer, F.L. Kearns, R.L. Silveira, B.C. Pollard, G. Dominick, R. Duman, K. El Omari, V. Mykhaylyk, A. Wagner, W.E. Michener, A. Amore, M.S. Skaf, M.F. Crowley, A.W. Thorne, C.W. Johnson, H.L. Woodcock, J.E. McGeehan, G.T. Beckham, Characterization and engineering of a plastic-degrading aromatic polyesterase, Proc. Natl. Acad. Sci. U. S. A. 115 (19) (2018) E4350–E4357, https://doi.org/10.1073/pnas.1718804115.
[33] J.C. Phillips, R. Braun, W. Wang, J. Gumbart, E. Tajkhorshid, E. Villa, C. Chipot, R.D. Skeel, L. Kalé, K. Schulten, Scalable molecular dynamics with NAMD, J. Comput. Chem. 26 (16) (2005) 1781–1802, https://doi.org/10.1002/jcc.20289.
[34] A.D. MacKerell, D. Bashford, M. Bellott, R.L. Dunbrack, J.D. Evanseck, M.J. Field, S. Fischer, J. Gao, H. Guo, S. Ha, D. Joseph-McCarthy, L. Kuchnir, K. Kuczera, F.T. Lau, C. Mattos, S. Michnick, T. Ngo, D.T. Nguyen, B. Prodhom, W.E. Reiher, B. Roux, M. Schlenkrich, J.C. Smith, R. Stote, J. Straub, M. Watanabe, J. Wiórkiewicz-Kuczera, D. Yin, M. Karplus, All-atom empirical potential for molecular modeling and dynamics studies of proteins, J. Phys. Chem. B 102 (18) (1998) 3586–3616, https://doi.org/10.1021/jp973084f.
[35] Q. Li, Y. Yan, X. Liu, Z. Zhang, J. Tian, N. Wu, Enhancing thermostability of a psychrophilic alpha-amylase by the structural energy optimization in the trajectories of molecular dynamics simulations, Int. J. Biol. Macromol. 142 (2020) 624–633, https://doi.org/10.1016/j.ijbiomac.2019.10.004.
[36] I. Taniguchi, S. Yoshida, K. Hiraga, K. Miyamoto, Y. Kimura, K. Oda, Biodegradation of PET: current status and application aspects, ACS Catal. 9 (5) (2019) 4089–4105, https://doi.org/10.1021/acscatal.8b05171.
[37] S. Kumar, G. Stecher, M. Li, C. Knyaz, K. Tamura, MEGA X: molecular evolutionary genetics analysis across computing platforms, Mol. Biol. Evol. 35(6) (2018) 1547–1549. doi:https://doi.org/10.1093/molbev/msy096.
[38] Y. Cui, Y. Chen, X. Liu, S. Dong, Y.e. Tian, Y. Qiao, R. Mitra, J. Han, C. Li, X. Han, W. Liu, Q. Chen, W. Du, S. Tang, H. Xiang, H. Liu, B. Wu, Computational redesign of a PETase for plastic biodegradation by the GRAPE strategy, bioRxiv (2019) 787069, https://doi.org/10.1101/787069.
[39] H. Mohamadi, B.P. Vandervalk, A. Raymond, S.D. Jackman, J. Chu, C.P. Breshears, I. Birol, DIDA: distributed indexing dispatched alignment, PLoS One 10 (4) (2015), e0126409, https://doi.org/10.1371/journal.pone.0126409.
[40] S. Henikoff, J.G. Henikoff, Position-based sequence weights, J. Mol. Biol. 243 (4) (1994) 574–578, https://doi.org/10.1016/0022-2836(94)90032-9.
[41] D.L. Wheeler, D.M. Church, A.E. Lash, D.D. Leipe, T.L. Madden, J.U. Pontius, G.D. Schuler, L.M. Schriml, T.A. Tatusova, L. Wagner, B.A. Rapp, Database resources of the National Center for Biotechnology Information: 2002 update, Nucleic Acids Res. 30(1) (2002) 13–16. doi:https://doi.org/10.1093/nar/30.1.13.
[42] A. Jacob, J. Lancaster, J. Buhler, B. Harris, R.D. Chamberlain, Mercury BLASTP: Accelerating protein sequence alignment, ACM trans. reconfigurable. Technol. Syst. 1 (2) (2008) 9–9. doi:https://doi.org/10.1145/1371579.1371581.
[43] F.J. Poelwijk, D.J. Kiviet, D.M. Weinreich, S.J. Tans, Empirical fitness landscapes reveal accessible evolutionary paths, Nature 445 (7126) (2007) 383–386, https://doi.org/10.1038/nature05451.
[44] P.A. Romero, F.H. Arnold, Exploring protein fitness landscapes by directed evolution, Nat. Rev. Mol. Cell Biol. 10 (12) (2009) 866–876, https://doi.org/10.1038/nrm2805.
[45] Q. Mu, Y. Cui, Y.e. Tian, M. Hu, Y. Tao, B. Wu, Thermostability improvement of the glucose oxidase from *Aspergillus niger* for efficient gluconic acid production via computational design, Int. J. Biol. Macromol. 136 (2019) 1060–1068. doi:https://doi.org/10.1016/j.ijbiomac.2019.06.094.
[46] D. Ribitsch, S. Heumann, E. Trotscha, E. Herrero Acero, K. Greimel, R. Leber, R. Birner-Gruenberger, S. Deller, I. Eiteljoerg, P. Remler, T. Weber, P. Siegert, K.-H. Maurer, I. Donelli, G. Freddi, H. Schwab, G.M. Guebitz, Hydrolysis of polyethyleneterephthalate by p-nitrobenzylesterase from *Bacillus subtilis*, Biotechnol. Prog. 27 (4) (2011) 951–960, https://doi.org/10.1002/btpr.610.
[47] D. Danso, C. Schmeisser, J. Chow, W. Zimmermann, R. Wei, C. Leggewie, X. Li, T. Hazen, W.R. Streit, New insights into the function and global distribution of polyethylene terephthalate (PET)-degrading bacteria and enzymes in marine and terrestrial metagenomes, Appl. Environ. Microbiol. 84(8) (2018) e02773-17. doi:https://doi.org/10.1128/aem.02773-17.
[48] D. Ribitsch, E.H. Acero, K. Greimel, A. Dellacher, S. Zitzenbacher, A. Marold, R.D. Rodriguez, G. Steinkellner, K. Gruber, H. Schwab, G.M. Guebitz, A new esterase from *Thermobifida halotolerans* hydrolyses polyethylene terephthalate (PET) and polylactic acid (PLA), Polymers (2012). doi:https://doi.org/10.3390/polym4010617.
[49] D. Ribitsch, E.H. Acero, K. Greimel, I. Eiteljoerg, E. Trotscha, G. Freddi, H. Schwab, G.M. Guebitz, Characterization of a new cutinase from *Thermobifida alba* for PET-surface hydrolysis, Biocatal. Biotransform. 30 (1) (2012) 2–9, https://doi.org/10.3109/10242422.2012.644435.
[50] A. Eberl, S. Heumann, T. Brückner, R. Araujo, A. Cavaco-Paulo, F. Kaufmann, W. Kroutil, G.M. Guebitz, Enzymatic surface hydrolysis of poly(ethylene terephthalate) and bis(benzoyloxyethyl) terephthalate by lipase and cutinase in the presence of surface active molecules, J. Biotechnol. 143 (3) (2009) 207–212, https://doi.org/10.1016/j.jbiotec.2009.07.008.
[51] F. Kawai, M. Oda, T. Tamashiro, T. Waku, N. Tanaka, M. Yamamoto, H. Mizushima, T. Miyakawa, M. Tanokura, A novel Ca2+−activated, thermostabilized polyesterase capable of hydrolyzing polyethylene terephthalate from Saccharomonospora viridis AHK190, Appl. Microbiol. Biotechnol. 98 (24) (2014) 10053–10064, https://doi.org/10.1007/s00253-014-5860-y.
[52] A.N. Shirke, C. White, J.A. Englaender, A. Zwarycz, G.L. Butterfoss, R.J. Linhardt, R.A. Gross, Stabilizing leaf and branch compost Cutinase (LCC) with glycosylation: mechanism and effect on PET hydrolysis, Biochemistry 57 (7) (2018) 1190–1200, https://doi.org/10.1021/acs.biochem.7b01189.
[53] S. Sulaiman, S. Yamato, E. Kanaya, J.-J. Kim, Y. Koga, K. Takano, S. Kanaya, Isolation of a novel cutinase homolog with polyethylene terephthalate-degrading activity from leaf-branch compost by using a metagenomic approach, Appl. Environ. Microbiol. 78 (5) (2012) 1556–1562, https://doi.org/10.1128/aem.06725-11.